A Comparative Study of Dual-slope Path Loss Model in Various Indoor Environments at 14 to 22 GHz

N. O. Oyie and T. J. O. Afullo
Discipline of Electrical, Electronic and Computer Engineering
University of KwaZulu-Natal, Durban 4041, South Africa

Abstract— Fifth generation wireless communication networks will demand massive bandwidth for high data rates. The millimeter wave frequency bands will play an important role in the 5G wireless networks due to the available huge chunk of bandwidth. Deployment of wireless networks will require an appropriate path loss model for site-specific environments such as indoor corridors. Structural design and building materials call for development of such models. This work presents a multi-frequency dual-slope large-scale path loss model based on measurements performed in two distinct indoor environments made of glass and concrete. Measurements were conducted at 14 to 22 GHz in typical indoor corridors using a costume-designed channel sounder based on Rohde and Schwarz SMF 100 A signal generator and FSIQ 40 signal analyzer with 120 MHz bandwidth for distances ranging 2 m to 24 m in line-of-sight and non-line-of-sight scenarios. The acquired measurement data of 36,000 directional power delay profiles for 18 transmitter-receiver combinations were analyzed to model a directional dual-slope path loss model for vertically polarized antennas. The directional dual-slope path loss was synthesized with consideration of propagation mechanisms such as reflection and diffraction effectively causing modal attenuation as the signal propagates along the corridor due to wave guiding effect. A breakpoint was established that demonstrates the effects of modal attenuation in a waveguide like corridor. The model was evaluated by performing a comparative analysis on the directional dual-slope path loss model on various indoor corridors with different structural design and materials with well-known alfa-beta-gamma model. The results were observed to give a better prediction of path loss at 14 to 22 GHz over ABG model as fitted to the measurement data. Moreover, the results show that the wave guiding effect is pronounced after the breakpoint due to both free space and multi-modal propagation.

1. INTRODUCTION

The consumer generated traffic and content has increasingly demanded wide bandwidth channels that will support high peak data rates of several Gigabits per second. Fifth generation (5G) millimeter wave (mmWave) bands promise the necessary bandwidth required for system design and deployment to support such throughput speeds for high-definition (HD) video, low latency content, and high data rate transfer and virtual interaction between people and machines [1]. Several standard bodies such as 3rd Generation Partnership Project (3GPP) and the International Telecommunication Union (ITU) are considering wideband channel models as a necessary first step in developing concepts such as beamforming and massive multiple-input multiple-output (MIMO) [2]. Large-scale path loss models should be accurate and intuitive based on repeatable measurements of channels behavior for real-world performance predictions and system design. Laws of physics that govern radio propagation should help in understanding path loss models for indoor corridor channels for the entire mmWave spectrum [3, 4].

Outdoor environments differ significantly from indoor environments in many ways. This makes indoor environments a special case of study under radio propagation. Consequently, signal power attenuation needs to consider the structural variations in the indoor environment. Additionally, multipath propagation along with usual fading and path loss due to distance, interference, shadowing, reflection, refraction, scattering, and penetration also impact on the received signal characteristics [5].

This paper presents a multi-frequency 14 GHz and 22 GHz directional dual slope (DS) path loss model that considers modal attenuation of signal power as it is guided in indoor corridors. The modal attenuation is as a result of multipath and propagating wave guiding effect in indoor corridors as opposed to shadowing fading. This model has been applied in path loss prediction for concrete and glass corridors and compared with alpha-beta-gamma (ABG) model. It is evident from the findings that a break point exists in the corridor that relates to the corridor dimension and frequency of transmission. DS model has been a popular generalization for decades with determination of model parameters via a linear regression of the experimental data. Corridors are

regarded as oversize dielectric waveguides with transversal dimensions much larger than wavelength, thus a number of modes are entirely involved in the propagation process. Certainly, propagating field in corridors is through superimposition of proper characteristics modes [6–8]. Moreover, the modal attenuation approach is mostly bounded by the fundamental mode which is least attenuated and occurs after the break point [9].

The rest of this paper is organized as follows: Description of measurement campaign is provided in Section 2. In Section 3, the break point is presented. Sections 4 and 5, analyze DS and ABG multi-frequency directional large scale path loss models. Section 6 presents the results and discussions of the findings of this work. Finally, this paper is concluded in Section 7.

2. MEASUREMENT CAMPAIGN

Measurements were performed within indoor corridors of the 5th and 2th floors (concrete and glass walled respectively) of the Discipline of Electrical, Electronic and Computer Engineering building, University of Kwa-Zulu Natal, South Africa. The environments were typical indoor corridors, a waveguide like structure with walls made of bricks and dry concrete, glass, wooden doors to offices, a staircase and an elevator (see Fig. 1). The channel sounder was based on Rohde and Schwarz SMF 100 A for radio frequency signal generation at the transmitter (Tx) side with a frequency range of 100 kHz to 22 GHz. Receiver (Rx) equipment was Rohde and Schwarz FSIQ 40 Signal Analyzer with a frequency range of 20 Hz to 40 GHz and maximum analysis bandwidth of 120 MHz. Measurement system consisted of a pair of wideband vertically polarized (V-V) directional pyramidal horn antennas with a 19.5 dBi gain, 3 dB beamwidth of 19.2° in elevation and 18.4° in azimuth and 22.1 dBi gain, 3 dB beamwidth of 13° in elevation and 15° in azimuth, at 14 GHz and 22 GHz respectively. A continuous wave was transmitted by the transmitter at 10 dBm and received power recorded at the receiver (Fig. 1) [10].

Figure 1: 14 GHz and 22 GHz multi-frequency V-V polarization DS and ABG directional path loss models for LOS and NLOS scenarios in indoor concrete and glass corridors. (a) Transmitter System. (b) Receiver System. (c) Glass Corridor.

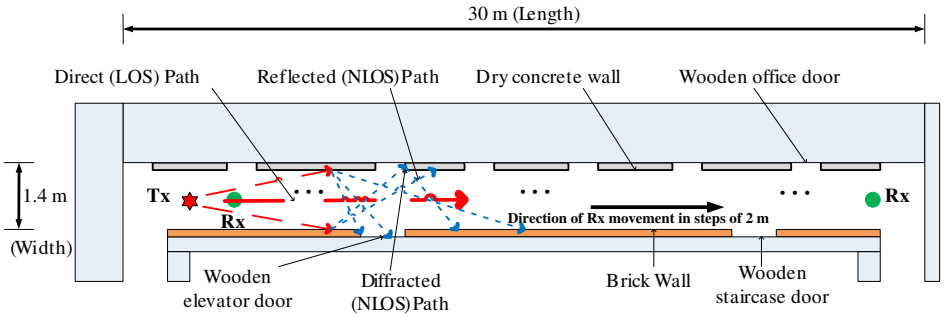

Figure 2: Floor plan of the indoor concrete corridor.

Line-of-sight (LOS) path loss was established for scenarios where Tx and Rx had no obstruction

between them and pointed at each other with alignment on boresight while the non-line-of-sight (NLOS) path loss was established in the environment where Tx and Rx had a clear LOS path to one another, but the antennas were out of alignment on boresight for each exclusive antenna pointing angles in every Tx and Rx combination [10, 11].

3. BREAK POINT

Different propagation mechanisms in corridors give rise to multipath, therefore, it is critical to establish how this phenomenon contributes to signal attenuation in indoor corridors. In this context, it is worth to note that diffraction plays a lesser role in the mmWave regime. Consequently, in NLOS scenario, the receiver will rely instead on ambient reflected paths [12–14]. This work establishes the break point using measurement data for concrete corridor. However, the glass corridor (10 m long) was observed to have no break point as at 14 GHz and 22 GHz frequency bands as provided for by Eq. (1). For concrete corridor, the break point was estimated at 12 m from Tx and expressed by Eq. (1):

$$d_{break} = \sqrt{\frac{a}{\lambda}} \tag{1}$$

where a is the maximum dimension of a corridor and λ is the signal wavelength.

4. DUAL SLOPE PATH LOSS MODEL

Wavefront divergence is the elemental aspect inherent in radio wave propagation with wavefront propagating spherically, its surface enlarges, consequently, its power density decreases with the square of the distance. Accordingly, the decrease in propagating signal power satisfies power-flux conservation. In guiding structures such as corridors, a quasi-2-D propagation with wave divergence proportional to the first power of distance should take place. However, higher path loss values with respect to the ideal cases are observed due to the presence of material losses [6].

The DS path loss model is therefore applied in these site-specific environments to model path loss with consideration of modal attenuation term $L_{m,n}$ [dB] (see Eq. (10)). This DS path loss model accounts for multipath propagation mechanisms in a corridor. It is observed in this paper that DS model is simple i.e., uses two instead of three modeling parameters as in ABG and accurate, hence suitable for general design and planning of network deployment in indoor environments.

The possible modes in a rectangular waveguide i.e., (m, n) modes can be geometrically described as a cluster of propagating wave into the corridor reflected on the vertical and horizontal walls with proper grazing angles $\phi_V^{m,n}$ and $\phi_H^{m,n}$ respectively. The electromagnetic field produced by these waves propagate progressively along the corridor's axis and on the contrary, a full standing wave in the xy plane, where the waves superimpose on each other to produce the (m, n) mode behavior. The grazing angles can be derived by the following relations [6]:

$$\sin\phi_H^{m,n} = \frac{\lambda \cdot n}{2h} \tag{2}$$

$$\sin\phi_V^{m,n} = \frac{\lambda \cdot m}{2w} \tag{3}$$

where λ is the wavelength, h is the height while w is the width of the corridor, n and m are x and y polarized mode numbers respectively.

From (2) and (3), the analytical expressions of distance between two consecutive bounces on the vertical $\Delta_V^{m,n}$ and horizontal $\Delta_H^{m,n}$ walls can be realized by means of trigonometrical considerations as [6]:

$$\Delta_V^{m,n} = \frac{w}{\tan(\phi_V^{m,n})} \cdot \sqrt{1 - \frac{\sin^2(\phi_H^{m,n})}{\cos^2(\phi_V^{m,n})}} \tag{4}$$

$$\Delta_H^{m,n} = \frac{h}{\tan(\phi_V^{m,n})} \cdot \sqrt{1 - \frac{\sin^2(\phi_V^{m,n})}{\cos^2(\phi_H^{m,n})}} \tag{5}$$

Equations (4) and (5) can be simplified as Eqs. (6) and (7) respectively, as modes with high grazing angle values can be considered negligible. In addition, the number of reflections on the vertical wall

($N_V^{m,n}$) and horizontal wall ($N_H^{m,n}$) given as Eqs. (8) and (9) respectively [6].

$$\Delta_V^{m,n} = \frac{w}{\tan(\phi_V^{m,n})} \cdot \cos\phi_H^{m,n} \tag{6}$$

$$\Delta_H^{m,n} = \frac{h}{\tan(\phi_H^{m,n})} \cdot \cos\phi_V^{m,n} \tag{7}$$

$$N_V^{m,n} = \frac{d}{\Delta_V^{m,n}} \tag{8}$$

$$N_H^{m,n} = \frac{d}{\Delta_H^{m,n}} \tag{9}$$

Finally, from (6)–(9), the *modal attenuation factor* (MAF) value, denoted by $L_{m,n}$ [dB], is given in (10). MAF is the power loss due to the multiple reflections on the mode wavefronts on the corridor walls. It is expressed as [6]:

$$\begin{aligned} L_{m,n}[\text{dB}] &= 10\left(N_V^{m,n} \cdot \log_{10}\frac{1}{|R_V(\phi_V^{m,n})|^2} + N_H^{m,n} \cdot \log_{10}\frac{1}{|R_H(\phi_H^{m,n})|^2}\right) \\ &= 10d\left(\frac{\tan(\phi_V^{m,n})}{w \cdot \cos(\phi_H^{m,n})} \cdot \log_{10}\frac{1}{|R_V(\phi_V^{m,n})|^2} + \frac{\tan(\phi_H^{m,n})}{h \cdot \cos(\phi_V^{m,n})} \cdot \log_{10}\frac{1}{|R_H(\phi_H^{m,n})|^2}\right) \end{aligned} \tag{10}$$

where R_V and R_H are the reflection coefficients of the vertical and horizontal walls respectively. We approximated the reflection coefficients in this paper as follows: floor (tile) as 0.1574, wall (brick) as 0.2037, wall (glass) as 0.4699, wall and ceiling (plasterboard) as 0.0743 [15]. The DS path loss model can be expressed as Eqs. (11) and (12):

$$PL^{DS}(d)[\text{dB}] = \begin{cases} PL_1^{DS}(d)[\text{dB}], & \text{for } d \le d_{break} \\ PL_2^{DS}(d)[\text{dB}], & \text{for } d \ge d_{break} \end{cases} \tag{11}$$

where

$$\begin{aligned} PL_1^{DS}(d)[\text{dB}] &= PL_{FS}(d_\circ) + 10 \times n_1 \times \log_{10}\left(\frac{d}{d_\circ}\right) + L_{m,n_1}(d), \\ PL_2^{DS}(d)[\text{dB}] &= PL_{break} + 10 \times n_2 \times \log_{10}\left(\frac{d}{d_{break}}\right) + L_{m,n_2}(d) \end{aligned}$$

and

$$PL_{break}[\text{dB}] = PL_{FS}(d_\circ) + 10 \times n_1 \times \log_{10}\left(\frac{d_{break}}{d_\circ}\right)$$

Therefore

$$PL^{DS}(d)[\text{dB}] = PL_1^{DS}(d)[\text{dB}] + PL_2^{DS}(d)[\text{dB}] + X_\sigma^{DS} \quad \text{for } d \ge d_\circ,\ d_\circ = 1\,\text{m} \tag{12}$$

where $PL^p(d)$ [dB] is the path loss at any distance d between Tx and Rx, $PL_1^p(d)$ [dB] and $PL_2^p(d)$ [dB] are the path losses before and after break point respectively, d_{break} is the break point while PL_{break} [dB] is the path loss at break point. Additionally, X_σ^p is a zero mean Gaussian random variable with standard deviation σ in dB, $L_{m,n_1}(d)$ and $L_{m,n_2}(d)$ are modal attenuations before and after the break point respectively.

DS path loss model is found by determination of the path loss exponent (PLE) n_1 (before break point)and n_2 (after break point) via the minimum mean square error (MMSE) method to minimize σ by simultaneously solving for n_1 and n_2 [10].

5. ALPHA-BETA-GAMMA PATH LOSS MODEL

ABG is a multi-frequency that includes a frequency dependent and distance-dependent terms in addition to PLE to describe the path loss at various frequencies. The ABG model can be expressed as Eq. (13):

$$PL^{ABG}(d)[\text{dB}] = 10\alpha\log_{10}\left(\frac{d}{d_\circ}\right) + \beta + 10\gamma\log_{10}\left(\frac{f}{1\,\text{GHz}}\right) + X_\sigma^{ABG} \quad \text{for } d \le d_\circ,\ d_\circ = 1\,\text{m} \tag{13}$$

where α and γ are coefficients that describe the distance and frequency-dependence on path loss, β is an optimized offset parameter that is devoid of physical meaning, f is the frequency in GHz, and X_{σ}^{ABG} is a zero mean Gaussian random variable with standard deviation σ in dB. The ABG model is solved via MMSE to minimize σ by simultaneously solving for α, β, and γ [11].

6. DISCUSSION

This paper presents multi-frequency directional DS and ABG path loss models as applied in indoor corridor environments (concrete and glass corridor). The DS model has a physical definition of the environment at $d_{\circ} = 1$ m as the reference distance for both LOS and NLOS models. The transmitted signal as received at the reference distance describes the physical characteristic of the channel. At millimeter, systems modeling use directional antennas for arbitrary directional pointing, beam steering, or beam combining techniques. Characterization of path loss considers antenna polarization. In this work, V-V polarization dataset for 14 GHz and 22 GHz was used to generate large-scale path loss models for indoor corridor environments. The Tx and Rx antennas were fixed at varying heights. Indoor concrete corridor's Tx antenna was fixed at 1.6 m and 2.3 m while Rx antenna was fixed at 1.6 m above the floor for both the Tx antenna heights. In indoor glass corridor, both Tx and Rx antennas were fixed at 1.6 m above the floor. Measurement distances were 24 m and 10 m for concrete and glass corridors, respectively, in steps of 2 m per measurement point.

Table 1 provides the multi-frequency directional V-V polarization at 14 GHz and 22 GHz path loss models measurement data for LOS and NLOS scenarios. PLE for DS model for Tx antenna height at 1.6 m are almost similar for concrete and glass corridors with an increase of 1 dB and 2 dB per decade of distance for LOS and NLOS respectively. In LOS, the PLE for DS (n_1 and n_2) and ABG (α) are less than 2 (free space PLE) as expected for an indoor environment with both Tx and Rx antennas fixed at 1.6 m for both concrete and glass corridors. The standard deviation for DS and ABG LOS are 1.7 and 1.3 respectively for both Tx and Rx fixed at 1.6 m. The α and β values vary over a wide range for ABG model that do not provide intuitive sense for different heights and scenarios.

Table 1: Regression Analysis of multi-frequency directional 14 GHz and 22 GHz DS and ABG models with Rx antenna height fixed at 1.6 m and Tx antenna height at 1.6 m and 2.3 m above the floor.

Env	Tx Height (m)	Rx Height (m)	DS Model						ABG Model							
			LOS			NLOS			LOS				NLOS			
			PLE			PLE			PLE				PLE			
			n_1	n_2	σ [dB]	n_1	n_2	σ [dB]	α	β	γ	σ [dB]	α	β	γ	σ [dB]
Conc. Corr.	1.6	1.6	1.7	1.4	1.7	2.5	0.1	4.8	1.4	20.0	3.7	1.3	0.5	50.3	2.6	0.5
	2.3	1.6	−0.9	0.6	3.2	−0.2	0.1	0.5	0.4	47.0	2.5	1.8	0.1	82.7	0.3	0.4
Glass Corr.	1.6	1.6	1.8	-	0.6	2.7	-	4.7	1.8	13.0	4.0	0.5	2.0	17.8	4.0	3.9

For Tx antenna height fixed at 1.6 m, the PLE reduces by 3 dB per decade of distance for DS LOS from before to after break point in concrete corridor. The PLE after break point for DS and ABG LOS are equal (i.e., 1.4). At Tx antenna height fixed at 2.3 m and elevation of −20°, the PLE for DS model for LOS and NLOS are −0.9 and −0.2 respectively, before the break point, because signal attenuates slowly as it is guided along the corridor up to break point as shown in Fig. 3. After the break point, PLE for NLOS DS model is 0.1 for both 1.6 m and 2.3 m Tx antenna heights, indicating that modal attenuation dominates after the break point as waves are guided in the corridor. Modal attenuation is typically low hence lower signal power loss per decade of distance after the break point.

Figures 3–5 show that ABG model has lower standard deviation for LOS and NLOS for both Tx antenna heights in all the indoor environments, which is in agreement with previous works [11]. It is notable in particular that DS model standard deviation is between 0.1 dB and 0.4 dB of the ABG model for LOS and NLOS respectively, in the indoor glass corridor environment, which is within typical measurement error. However, for indoor concrete corridor in both the scenarios, the

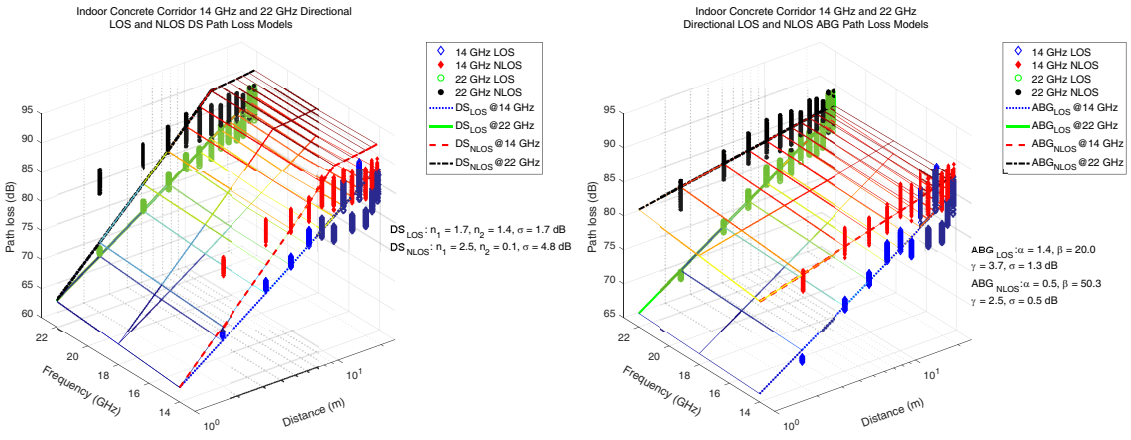

Figure 3: 14 GHz and 22 GHz multi-frequency V-V polarization DS and ABG directional path loss models for LOS and NLOS scenarios in indoor concrete corridor environment. (a) DS directional path loss model for LOS and NLOS and scatter plot. (b) ABG directional path loss model for LOS and NLOS and scatter plot.

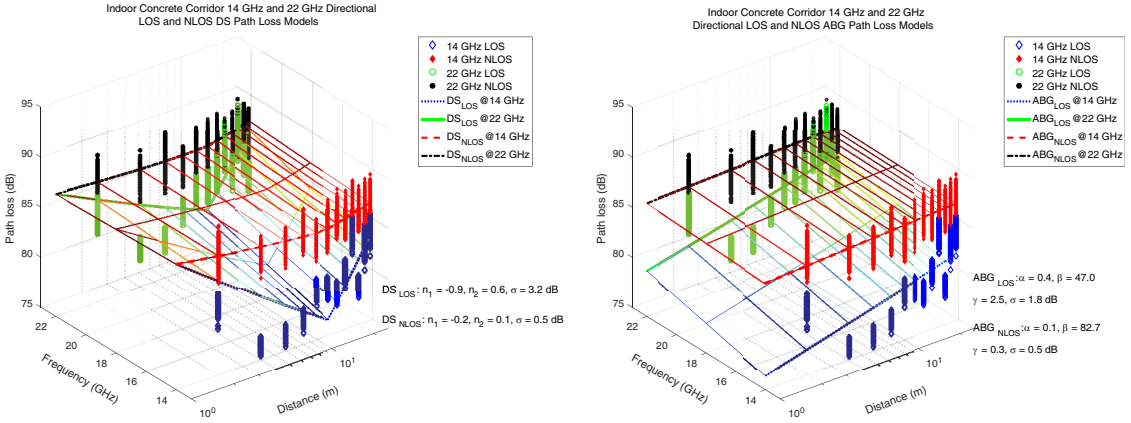

Figure 4: 14 GHz and 22 GHz multi-frequency V-V polarization DS and ABG directional path loss models for LOS and NLOS scenarios in indoor concrete corridor environment. (a) DS directional path loss model for LOS and NLOS and scatter plot. (b) ABG directional path loss model for LOS and NLOS and scatter plot.

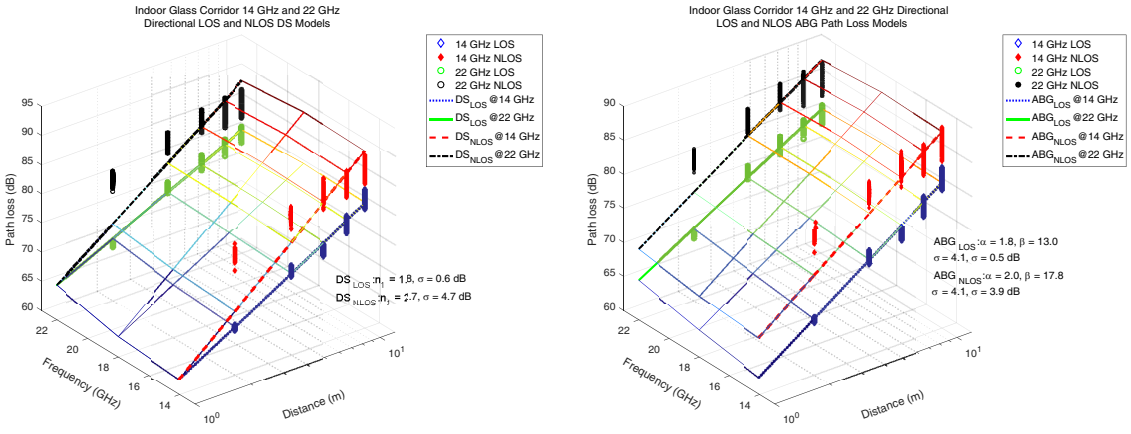

Figure 5: 14 GHz and 22 GHz multi-frequency V-V polarization DS and ABG directional path loss models for LOS and NLOS scenarios in indoor glass corridor environment. (a) DS directional path loss model for LOS and NLOS and scatter plot. (b) ABG directional path loss model for LOS and NLOS and scatter plot.

standard deviation for the ABG model is up to 4.3 dB smaller than DS model. ABG model uses three modeling parameters that vary over a wide range without intuition of the physics.

7. CONCLUSION

A linear regression approach is employed in determination of the predicted path loss for DS and ABG model. From Table 1, DS and ABG have two and three modeling parameters, respectively. The DS model is found to be stable with intuitive physical sense. However, the ABG model is sensitive and unstable as its parameters (β and γ) vary over a wide range of values without intuitive sense, thus making it less suitable for application.

Our results show that: 1) Beyond the break point, the indoor corridor environment acts as a waveguide with transmitted signal power attenuation dominated by modal attenuation. 2) Free space attenuation dominates the signal power loss up to the break point that is determined by Eq. (1), whereas modal attenuation takes effect after break point as provided for by the PLE in Table 1. 3) The height of transmitting antenna has no effect on the location of break point within a corridor. 4) The maximum observable PLE in both the indoor corridors are 1.8 and 2.7 for LOS and NLOS respectively, that is supported by similar values in previous works [11]. 5) More importantly, the statistical DS path loss model fits well in measurement data and appears extendable to other enclosed structures such as tunnels and building corridors by adjusting the parameter values.

This work shows that ABG model is optimistic in path loss prediction in all scenarios and environments with three modeling parameters that have no intuitive sense. In addition, it is sensitive and unstable hence prone to inaccuracy. The main cause of this is parameter β that has no physical reference hence floating. However, DS uses two and one modeling parameters for indoor environments with and without break points respectively. Additionally, it considers the wave guiding effect in the waveguide-like structures. The main cause of signal attenuation after the break point is modal attenuation that is well factored in the model.

REFERENCES

1. Lota, J., S. Sun, T. S. Rappaport, and A. Demosthenous, "5G uniform linear arrays with beamforming and spatial multiplexing at 28, 37, 64, and 71 GHz for outdoor urban communication: A two-level approach," *IEEE Transactions on Vehicular Technology*, Vol. 66, No. 11, 9972–9985, Nov. 2017, doi: 10.1109/TVT.2017.2741260.
2. Rappaport, T. S., S. Sun, and S. Mansoor, "5G channel model with improved accuracy and efficiency in mmWave bands," *IEEE 5G Tech Focus*, Vol. 1, No. 1, Mar. 2017.
3. Ertel, R. B., P. Cardieri, K. W. Sowerby, T. S. Rappaport, and J. H. Reed, "Overview of spatial channel models for antenna array communication systems," *IEEE Personal Communications*, Vol. 5, No. 1, 10–22, Feb. 1998, doi: 10.1109/98.656151.
4. Samimi, M. K., S. Sun, T. S. Rappaport, "MIMO channel modeling and capacity analysis for 5G millimeter-wave wireless systems," *the 10th European Conference on Antennas and Propagation (EuCAP 016)*, Apr. 2016.
5. Rath, H. K., S. Timmadasari, B. Panigrahi, and A. Simha, "Realistic indoor path loss modeling for regular WiFi operations in India," *23rd National Conf. on Comm. (NCC)*, Vol. 1, 1–6, Mar. 2–4, 2017.
6. Fushini, F. and G. Falciasecca, "A mixed rays-modes approach to the propagation in real road and railway tunnels," *IEEE Transactions on Antennas and Propagation*, Vol. 60, No. 2, 1095–1105, Feb. 2012.
7. Dudley, D., M. Lienard, S. F. Mahmoud, and P. Degaque, "Wireless propagation in tunnels," *IEEE Antennas Propag. Mag.*, Vol. 49, No. 2, 11–26, Apr. 2007.
8. Sun, Z. and I. F. Akyldiz, "Channel modeling and analysis for wireless networks in underground mines and road tunnels," *IEEE Trans. Commun.*, Vol. 58, No. 6, 1758–1768, Jun. 2010.
9. Emslie, A. G., R. L. Lagace, and P. F. Strong, "Theory of the propagation of UHF radio waves in coal mine tunnels," *IEEE Trans. Antennas Prop.*, Vol. 23, No. 2 192–205, Mar. 1975.
10. Oyie, N. O. and T. J. O. Afullo, "Measurements and analysis of large-scale path loss model at 14 and 22 GHz in indoor corridor," *IEEE Access*, Vol. 6, 17205–17214, 2018, doi: 10.1109/ACCESS.2018.2802038.
11. McCartney, G., T. S. Rappaport, S. Sun, and S. Deng, "Indoor office wideband millimetre-wave propagation measurements and channel models at 28 and 73 GHz for ultra-dense 5G wireless networks," *IEEE Access*, Vol. 3, 2388–2424, Dec. 2015.

12. Senic, J., C. Gentile, P. B. Papazian, K. A. Remley, and J. K. Choi, "Analysis of E-band path loss and propagation mechanisms in the indoor environment," *IEEE Transactions on Antennas and Propagation*, Vol. PP, No. 99, 1–12, doi: 10.1109/TAP.2017.2722876.
13. Rappaport, T. S., R. W. Heath, Jr., R. C. Daniels, and J. N. Murdock, *Millimeter Wave Wireless Communications*, Englewood Cliffs, Prentice Hall, NJ, USA, 2015.
14. Deng, S., G. R. MacCartney, Jr., and T. S. Rappaport, "Indoor and outdoor 5G diffraction measurements and models at 10, 20, and 26 GHz," *IEEE Global Communications Conf.*, Dec. 4–8, 2016, 10.1109/GLOCOM.2016.7841898.
15. Sato, K., et al., "Measurements of reflection characteristics and refractive indices of interior construction materials in millimeter-wave bands," *IEEE 45th Vehicular Technology Conference Countdown to the Wireless Twenty-First Century*, Vol. 1, 449–453, Chicago, IL, 1995, 10.1109/VETEC.1995.504907.